

# Method for Detecting (Anti-)deuterons from the LHCb Experiment

Isabel Weeden  
Supervisors: Ulrik Egede, Eliot Walton

PHS2350 Research Project

November 7, 2022

## Abstract

The annihilation of dark matter may produce detectable Standard Model particles and one possible particle is the anti-deuteron. By measuring (anti-)deuterons from proton-proton collisions using the LHCb detector, the properties of dark matter may be further understood. To identify a particle at the LHCb detector we need both its momentum and velocity to determine its mass. Previous work has shown that (anti-)deuterons cannot be measured directly, nor can they be measured collectively due to background and how rare they are. In this project, a method is devised to interpolate and estimate the background by looking at hypothetical masses above and below the proton mass, this showed the protons to be easily distinguished from the background, suggesting that the same method could be applied to (anti-)deuterons.

## Acknowledgements

I would like to show my appreciation towards Professor Ulrik Egede, for giving me the opportunity to take on this project, allowing me to further my understanding of particle physics and providing me with invaluable experience in research. I would also like to thank Eliot Walton for guiding me through the project and for her time spent helping me overcome challenges.

# Contents

<b>1</b>	<b>Introduction</b>	<b>1</b>
1.1	Particle Physics and the Standard Model . . . . .	1
1.2	Dark Matter . . . . .	1
1.3	Project Motivation . . . . .	2
<b>2</b>	<b>Background</b>	<b>2</b>
2.1	Deuteron Formation . . . . .	2
2.2	Previous Deuteron Measurements . . . . .	3
<b>3</b>	<b>The LHCb Detector</b>	<b>4</b>
3.1	Detecting Deuterons . . . . .	4
3.2	Tracking System . . . . .	4
3.3	Cherenkov Radiation . . . . .	4
3.4	RICH Detectors . . . . .	6
3.5	Previous Work at the LHCb Experiment . . . . .	7
<b>4</b>	<b>Experimental Method and Results</b>	<b>7</b>
4.1	The Data and Delta Log Likelihood . . . . .	7
4.2	Changing Mass Hypothesis . . . . .	8
4.3	Results . . . . .	8
<b>5</b>	<b>Conclusion</b>	<b>10</b>
<b>6</b>	<b>Future Work</b>	<b>11</b>

# 1 Introduction

This report presents the results of a second year research project undertaken in 2022. In this project a method was devised to detect (anti-)deuterons from the LHCb experiment from 2018 data, in the hopes better understand the properties of dark matter and to potentially indirectly detect it. Section 1 illustrates the motivation for the project, while Section 2 provides some background on deuterons and previous work. Section 3 details the nature of the LHCb detector, with Section 4 presenting the method, results and discussion of findings.

## 1.1 Particle Physics and the Standard Model

The Standard Model of particles consists of leptons, quarks and the force carrying bosons. In the Standard Model, particles are described by quantum fields, which are characterised by the exchange of virtual particles, these virtual particles are photons in the case of quantum electrodynamics, and gluons for quantum chromodynamics [3]. Quantum electrodynamics describes how light and matter interact by the electromagnetic force, while quantum chromodynamics describes the strong force, the force which binds quarks. There is also the Weak force, a short range force which acts between nucleons, which is mediated by massive W and Z bosons [3].

While the Standard Model does well at describing electromagnetism and the strong and weak nuclear forces, it does not give us an explanation for the existence of dark matter, which is invisible matter that makes up the majority of matter in the Universe compared to normal luminous matter. The issue with dark matter is that it cannot be directly detected, this is because dark matter does not interact with the electromagnetic force [4], so it cannot interact with light, making it hard to further understand its properties and its production.

## 1.2 Dark Matter

Dark matter was first proposed to explain the rotation curves of galaxies, which were found to not have as much mass as had been predicted, the existence of dark matter has further been suggested by the measurements of gravitational lensing [5], which is the bending of light due to the presence of matter. Dark matter makes up most of the matter in the universe, though it is not understood exactly what it is, nor has it been directly detected.

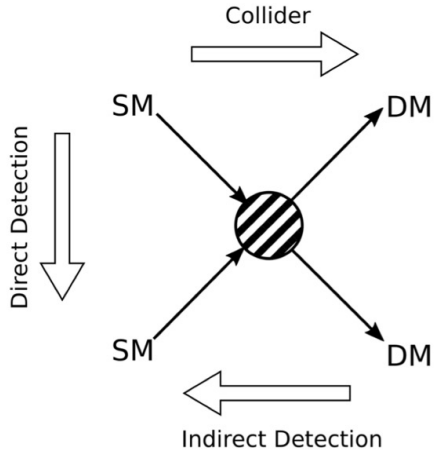


Figure 1: Schematic of dark matter (DM) annihilation and production from Standard Model particles (SM). Reproduced from Ref [9].

It has been proposed that the annihilation of dark matter and anti-dark matter particles occurred rapidly at the beginning of the universe, but has since slowed. Dark matter may be produced by the

annihilation of Standard Model particles [6], as shown in Figure 1. If this is the case then the annihilation of dark matter and anti-dark matter particles may produce detectable Standard Model particles. It has been proposed that this would occur through a portal particle, a particle which couples both dark matter and normal matter to allow energy to be exchanged between them, maintaining thermal equilibrium [7]. This is required as gravity is too weak to exchange the energy needed. This portal particle would then decay into Standard Model particles, which may then travel through the galaxy as cosmic rays and potentially be able to be detected by space-based instruments in the future.

Annihilation of dark matter may produce particles such as anti-deuterons, anti-protons and positrons, from the decay of a portal particle. A deuteron is the nucleus of deuterium, consisting of a bound state of a proton and a neutron. An anti-deuteron is the anti-matter particle of a deuteron. One proposed portal particle candidate is the Higgs boson, which is responsible for giving particles their mass [7]. The Higgs Boson is suitable as it already exists in the Standard Model, the dominant decay of the Higgs Boson produces quarks and because dark matter is massive, it seems a reasonable candidate for the portal particle. However, the Higgs boson has not yet been successfully demonstrated to be such a portal particle [7]. There have also been attempts to produce dark matter using the portal particle from the annihilation of Standard Model particles [8], though it has yet to be demonstrated successfully.

The possible production of anti-deuterons from dark matter annihilation may provide a good candidate for trying to indirectly detect dark matter. Anti-deuterons may be suitable because they are stable, and sufficiently rare that they could be distinguished from background in cosmic rays. As cosmic rays consist of high energy protons, cosmic ray collisions may produce anti-deuterons as well, though this cannot be readily detected.

### 1.3 Project Motivation

The motivation of this project is to better understand how (anti-)deuterons can be formed from proton-proton collisions within the Standard Model, to then give us an idea of how anti-deuterons could be formed from dark matter annihilation. If we are able measure how many anti-deuterons are produced from proton-proton collisions, this will then tell us what we should be looking for when trying to detect dark matter annihilation signatures in cosmic radiation using space-based instruments.

One way in which we can measure proton-proton collisions more readily is with the Large Hadron Collider (LHC), which is a particle accelerator which accelerates protons to relativistic speeds and measures the products after the collision [10]. The LHCb detector, which is one of the main detectors at the LHC, in particular specialises in differences between matter and anti-matter by studying bottom quarks. Thus if we can detect (anti-)deuterons from the LHCb detector and eventually find a way to count them, we may have better hope for understanding the properties of dark matter.

However because (anti-)deuterons are so rare, it has shown to be hard to detect them directly [1]. One possible solution to this was by devising a method to collectively measure (anti-)deuterons using a Statistical approach with the data from LHCb detector, though it was found that the (anti-)deuterons could not be distinguished from background given how rare they are and the size of the current data set [2]. The method in this project consists of interpolating and getting an estimate of the background that is making it so hard to detect (anti-)deuterons, by finding the background first in relation to protons, with the hopes to then apply the same method to the rarer (anti-)deuterons.

## 2 Background

### 2.1 Deuteron Formation

As deuterons and anti-deuterons are produced in pairs at the same rate, we get equivalent measurements for deuterons as we do for anti-deuterons. There are a few models of how deuterons/anti-deuterons may be formed from proton-proton collisions. One of which is the coalescence model, this is where a proton and a neutron come together a distance away from their point of origin, as shown

in Figure 2, with the two particles binding if their collective momentum is less than the coalescence momentum [11]. However, one issue with the Coalescence model is that four-momentum is not conserved, thus making it contradict the Standard Model. One way to get around this is by introducing a photon that is produced along with the deuteron. Another issue with the coalescence method is that the coalescence momentum varies depending on the energy scale [11], making it hard to predict the formation of a deuteron.

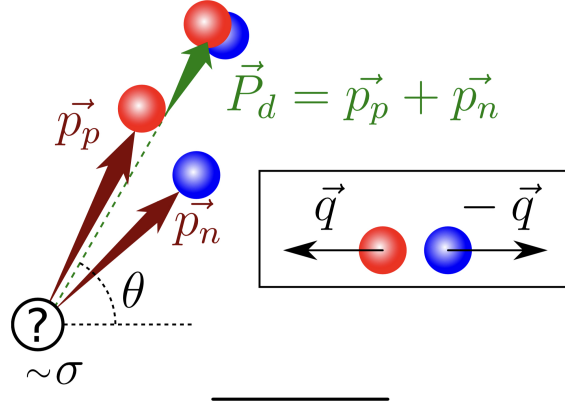


Figure 2: Schematic of the coalescence model showing a proton and a neutron producing a deuteron. Where  $p_p, p_n$  and  $P_d$  denote the momentum of the proton, neutron and deuteron respectively. Reproduced from Ref[11].

Another production mechanism for deuterons is the cross-section model, which allows deuterons to be formed from other particles in high energy events, not necessarily just a proton and a neutron [12]. Such possible production processes are shown in Table 1. While more complicated than the coalescence method, the cross-section model is consistent with the Standard Model unlike the coalescence method, as four-momentum is conserved in each of the eight processes in Table 1. Despite these conceptual advantages, it is still not clear whether the cross-section or Coalescence model is the best model for deuteron production, as they both are able to be fitted closely to data.

- |   |   |
|---|---|
| 1) $\bar{p}\bar{n} \rightarrow \bar{d}\gamma$     | 5) $\bar{p}\bar{p} \rightarrow \bar{d}\pi^-$      |
| 2) $\bar{p}\bar{n} \rightarrow \bar{d}\pi^0$      | 6) $\bar{p}\bar{p} \rightarrow \bar{d}\pi^-\pi^0$ |
| 3) $\bar{p}\bar{n} \rightarrow \bar{d}\pi^+\pi^-$ | 7) $\bar{n}\bar{n} \rightarrow \bar{d}\pi^+$      |
| 4) $\bar{p}\bar{n} \rightarrow \bar{d}\pi^0\pi^0$ | 8) $\bar{n}\bar{n} \rightarrow \bar{d}\pi^+\pi^0$ |

Table 1: Possible processes for deuteron production by the Cross-section Model, where  $\pi$  are pions with charges of 1,-1 and zero. Adapted from Ref[12].

## 2.2 Previous Deuteron Measurements

Previous work suggests that deuterons can be produced from collisions of relativistic heavy ions [13]. Having more energy than proton-proton collisions, Pb-Pb collisions are more likely to produce a higher abundance of (anti-)deuterons compared to collisions of lighter particles such as proton-proton collisions. The ALICE (A Large Ion Collider Experiment) Collaboration has shown promise that (anti-)deuterons can be measured from Pb-Pb collisions at  $\sqrt{s_{NN}} = 2.76$  TeV, and in proton-Pb collisions at  $\sqrt{s_{NN}} = 5.02$  TeV [13], where  $\sqrt{s}$  is the centre of mass energy. The ALICE detector at the Centre for European Nuclear Research (CERN), is a detector which studies heavy-ion collisions as well proton-proton collisions, at extreme energy densities [15].

By looking at the multiplicity and transverse momentum of light nuclei, the ALICE collaboration has also shown that (anti-)deuterons can be measured from proton-proton collisions at  $\sqrt{s} = 13TeV$  [14], with a similar yield for the deuterons as seen in proton-Pb collisions. It showed that at lower

energies that the Coalescence and Cross-section models both showed similar results, though at higher energies, the cross-section model appeared to fit the data more closely [14].

Further attempts at measuring deuterons with the LHCb detector are discussed in Section 3.5.

### 3 The LHCb Detector

The LHCb detector consists of several sub-detectors designed to identify different particles [16], as shown in Figure 3. The proton-proton collisions occur in the Vertex Locator (located on left-hand side of Figure 3), with the particles that are produced passing through the Ring Imaging Cherenkov (RICH) detectors. There is also a magnet in between the RICH detectors which bends the path of the particle, to allow the momentum and charge of the particle to be reconstructed [16].

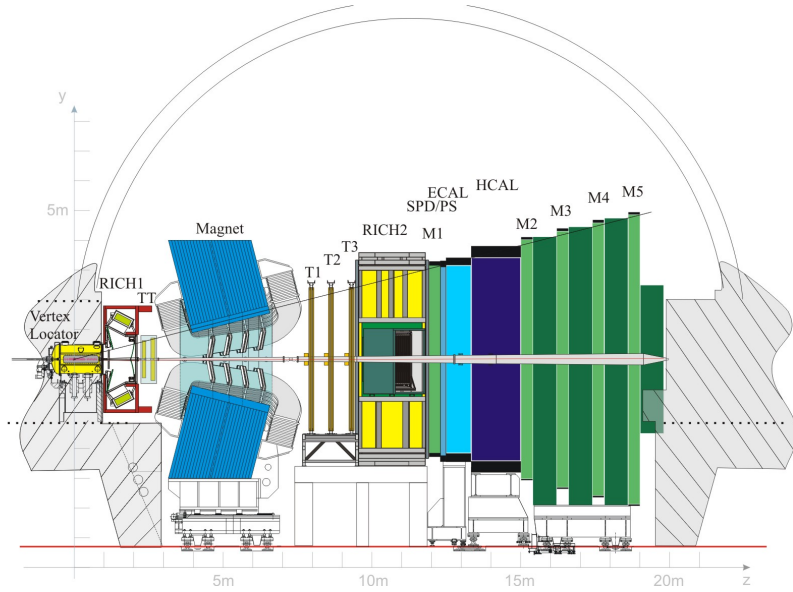


Figure 3: Diagram of the LHCb detector at CERN. Reproduced from Ref[16].

#### 3.1 Detecting Deuterons

Particles in the LHCb detector can be identified if we have both the momentum and the velocity of the particle. The momentum of the particle can be obtained by sending it through a magnetic field, produced by the magnet in between the two RICH detectors, and measure the radius of curvature of the particle as it is deflected. While the particles velocity can be determined from the Cherenkov radiation measured through the RICH detectors.

#### 3.2 Tracking System

For the momentum to be measured, tracking is used to measure the curvature of the charged particles through the magnetic field. This involves the use of tracking stations, placed before and after the magnet, which use silicon trackers and straw tubes. The silicon trackers are used to maximise the spatial resolution, while the gaseous straw detectors are used to determine the trajectory of the particles. These tubes provide a drift time of 50.0 ns [2].

#### 3.3 Cherenkov Radiation

The velocity of the particle is obtained from its Cherenkov radiation. Cherenkov radiation is electromagnetic radiation that is produced when a particle, travelling at relativistic speeds, travels through

a dielectric medium of refractive index  $n$  [17].

As the dielectric media has a specific refractive index, the speed of a particle travelling through the media changes, with each media having its associated speed of light. If the speed of this particle in the media exceeds this associated speed of light in the media, without travelling faster than the speed of light in a vacuum, then Cherenkov radiation is produced [17].

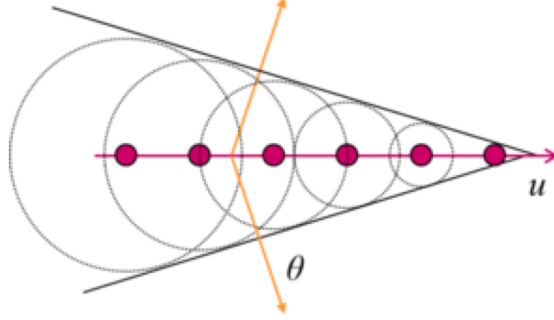


Figure 4: Schematic of Cherenkov radiation produced in a cone like shape around particle with velocity  $u$ , and the angle with respect to the direction of the particles velocity, this angle is much smaller than depicted in the diagram. Reproduced from Ref[18].

Cherenkov radiation is produced in a cone-like shape as shown in Figure 4, where the shape appears like wave fronts. If the angle  $\theta_{ch}$  at which the radiation is produced with respect to the direction of the particles velocity ( $u$ ) is measured, then the velocity of the particle can then be obtained, such that,

$$\cos(\theta_{ch}) = \frac{1}{n\beta}, \quad (1)$$

where  $\beta$  is velocity of the particle in terms of the speed of light  $c$  and  $n$  is the refractive index of the dielectric medium.

Particles will begin to radiate Cherenkov radiation when they travel fast enough that  $\beta_t > \frac{1}{n}$ , this is the threshold velocity [19]. As the velocity of the particle increases, it continues to radiate, however as the saturation angle is approached [10], when

$$\theta_{sat} = \arccos\left(\frac{1}{n}\right), \quad (2)$$

which occurs when  $\beta$  is roughly 1, the particle will no longer be able to be identified as it cannot be distinguished from other particles. So while two different particles may be travelling at the same speed, because they have different masses they will begin radiating at different momenta. Thus, we should look in a momentum region above the threshold velocity, and below the saturation angle to try and detect a given particle.

Figure 5 shows the regions based on the threshold velocity and saturation angle where we expect protons, pions, kaons and deuterons to be most easily detected. For protons it appears to be around 18-24 GeV, for kaons about 9-12 GeV and deuterons around 36-52 GeV.

With both the momentum of the particle obtained by sending it through a magnetic field, and the velocity of the particle from the Cherenkov radiation, the particles mass is then able to be determined by,

$$E^2 = p^2 + m^2, \quad (3)$$

where  $E$  is the energy of the particle,  $p$  is the momentum and  $m$  is the particles mass. As the masses of the particles are accurately known, the particle is then able to be identified from its mass.

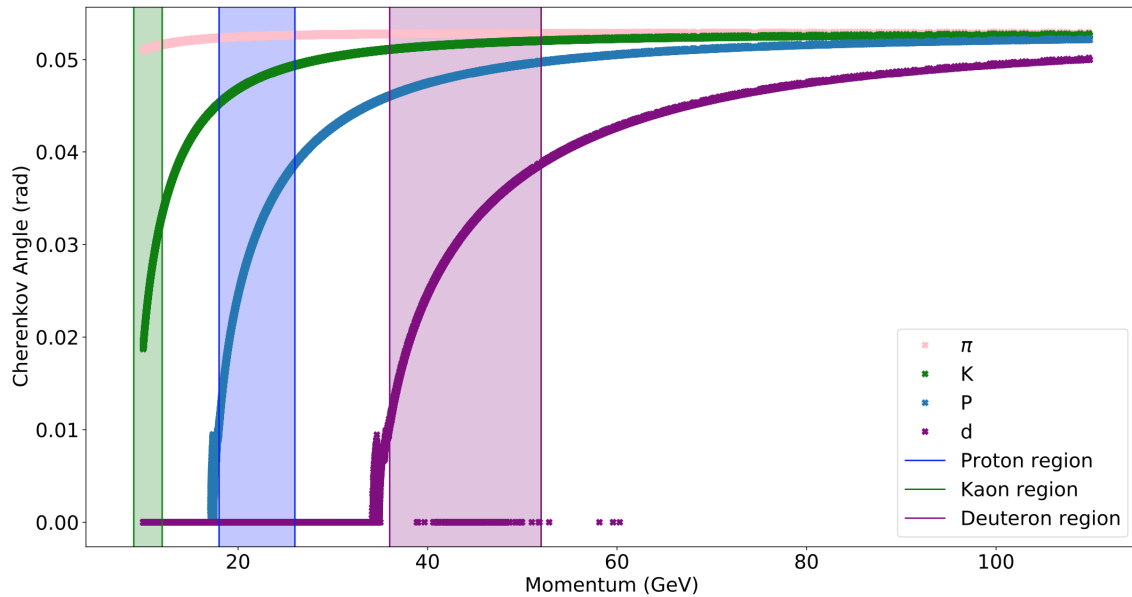


Figure 5: Cherenkov angle in radians versus momentum in GeV for pions, protons, kaons and deuterons, with their expected momentum regions highlighted. Adapted from Ref[2].

### 3.4 RICH Detectors

The Ring Imaging Cherenkov (RICH) detectors in the LHCb experiment consists of two detector, RICH 1 and RICH 2, which contain layers of  $C_4F_{10}$  and  $CF_4$  respectively [10]. The particle is sent through these detectors which have specific refractive indices, allowing them to produce Cherenkov radiation if their speed surpasses the speed of light in the media.

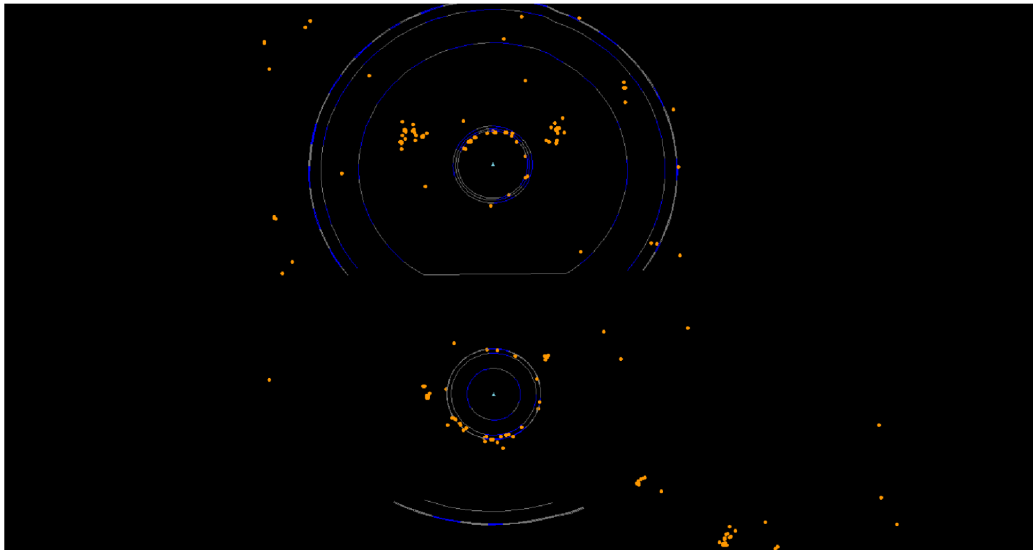


Figure 6: Example of a  $pp \rightarrow pp\mu^+\mu^-$  event displayed on HPD plane for RICH 1 from 2011 data. The particle is shown in the centre with the orange points showing the hits (photons) from the Cherenkov radiation, the blue rings are the expected ring radii for a given particle depending on its mass. Reproduced from Ref[10].

The photons produced from the Cherenkov radiation are reflected through two mirrors, allowing

them to form rings on the Hybrid Photo Detector (HPD) plane [10]. The Cherenkov rings produced on the detector are dependent on the mass of the particle being detected, such that the ring radii of the photons is proportional to the Cherenkov angle. However, background photons are also gathered by the detector, making it hard to identify the rings of the particle being detected, especially for rarer particles.

### 3.5 Previous Work at the LHCb Experiment

Deuterons were first attempted to be measured from the LHCb in 2019 case-by-case, by searching for individual deuteron measurements from 2018 data [1]. This was done by looking at the expected ring radii for the deuteron mass. However, this was not successful due to the rarity of the deuterons. As shown in Figure 6, the photons supposedly produced from the deuterons are so rare that random background photons that look like deuterons are more common.

Based on this, another method to try and detect deuterons from the same data was developed. This was done by forming a distribution out of the distance from each track to every photon and then looking for structures in this distribution which most likely correspond to Cherenkov rings. The statistically significant measurements that were close enough to the deuteron mass radius were selected [2], such that they have a higher probability of corresponding to a deuteron. This was done by using the mass ratio of kaons to protons, as this is almost equivalent to the mass ratio of protons to deuterons. It was found that the ratio of protons to kaons was  $0.73 \pm 0.03$  [2], which is within  $2\sigma$  of the value by the case-by-case of 0.78, based on Ref [1]. However, when applied to the deuterons, it was found that the deuterons could not be distinguished from background photons, with a factor of 2500 more data needed to produce a statistically significant result.

## 4 Experimental Method and Results

The prospect that deuterons cannot be measured both directly and collectively due to background photons has motivated this project, where we are looking more closely at the background to see if deuterons can be distinguished.

### 4.1 The Data and Delta Log Likelihood

The data being used is the same 2018 data from the LHCb detector, consisting of all the charged particles detected from a few seconds of proton-proton collisions. In this project, the data is being used in the form of likelihoods. This consists of the product of the probabilities that a specific Cherenkov photon ring corresponds to a particular particle by how close that photon is to the radii for that given particle. For example, the likelihood for a proton is the probability that a given photon ring is close enough to the proton mass radius, multiplied by the probability for another photon and so on. The likelihood can also be obtained for kaons, pions and deuterons.

As most of the particles detected by the LHCb detector are pions, we expect that most of the photons will correspond to pions, because of this, we take the ratio of the likelihood of a given particle compared to a pion, that way we avoid the issue that every particle will most likely correspond to a pion compared to any other particle. The log of this ratio of the likelihoods is also taken, such that we obtain for the likelihood of a proton compared to a pion,

$$\Delta LL = LL_p - LL_\pi, \tag{4}$$

where  $LL_p$  is the log of the likelihood for a proton, and  $LL_\pi$  is the log of the likelihood for a pion. This gives us the delta log likelihood  $\Delta LL$ , we take the log because the individual probabilities that make up the likelihood will consist of many small numbers close to zero, so it is better to take the sum of them rather than multiply them as it is more intuitive. Thus we expect for a track which corresponds to a proton, that the  $\Delta LL$  will be larger than zero, while for a pion, or any other particle that is not a proton, we expect the  $\Delta LL$  to be less than zero.

The  $\Delta LL$  values for each of the particles are obtained in the momentum region of 2-100 GeV as this is where the RICH detectors measure the particles. Thus we will be looking at the  $\Delta LL$  for a given particle in a region above where we expect the particle to start radiating Cherenkov radiation, and below the saturation, based on Figure 5.

## 4.2 Changing Mass Hypothesis

The method used in this project to try to get an idea of the background photons, is to look at masses above and below the proton mass. Protons are being used to validate the method as they are about 1000 times more common than deuterons.

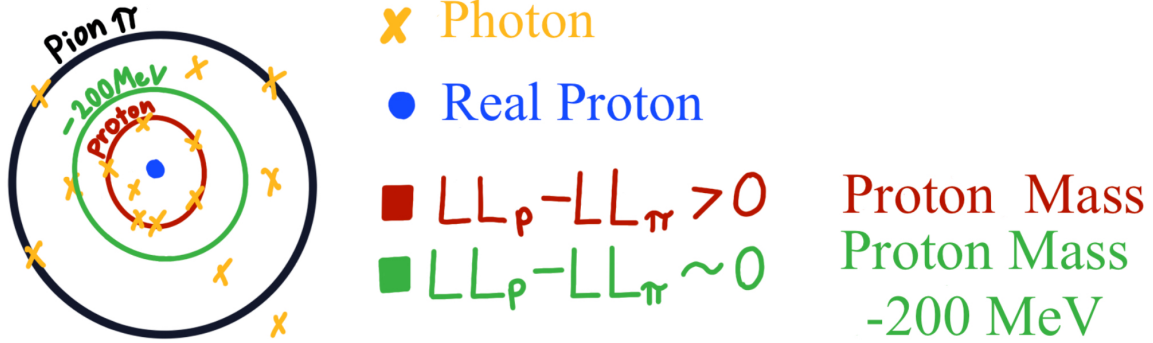


Figure 7: Example diagram of the changed mass hypothesis ring for 200 MeV below the proton mass, compared to the expected ring radii for protons and pions for a real proton. For a real proton, more photons (orange) are expected to be at the proton mass radius, resulting in a higher  $\Delta LL$ , while for the changed mass it is expected to be around zero as there will be no particle there.

This idea of changing the mass hypothesis involves selecting a momentum and velocity to give us a certain hypothetical mass. This then gives us a hypothetical Cherenkov ring radius, where we expect there to be no particles and thus no photons from a particle. This will then give us an idea of the background, as we expect only background photons to be detected at this radii, similar to what is shown in Figure 6. In natural units, the mass of a proton is 938.3 MeV, the changed masses were arbitrarily chosen to be 200 MeV above and below the proton mass, and 400 MeV above the proton mass. A mass of 400 MeV below the proton was not chosen as this would have been too close to the kaon mass which is 493.68 MeV.

With these changed masses, we can then look at the  $\Delta LL$  for protons, at the expected proton mass, and compare this to the  $\Delta LL$  for protons at the changed masses. An example of what changing the mass involves with the different Cherenkov rings is shown in Figure 7 for 200 MeV below the proton mass, with the expected  $\Delta LL$  at the changed mass and the proton mass. Kaons were also used as a control variable such that the  $\Delta LL$  was obtained for kaons at the expected proton mass and at the changed masses where,

$$\Delta LL = LL_k - LL_\pi. \quad (5)$$

We expect that the  $\Delta LL$  for the kaons should remain unchanged by the alterations to the proton mass hypothesis, given that we are not looking at the kaon mass radius.

## 4.3 Results

The data consists of the number of tracks, which corresponds to the number of charged particles being detected, for the  $\Delta LL$  for the kaons and protons at the proton mass and at the masses of 200 MeV above and below the proton mass, and 400 MeV above the proton mass. The tracks were only selected for the momentum region of 18-24 GeV for the protons, based on where protons start to radiate Cherenkov radiation and thus be detected shown in Figure 5. If we were to look at the data over the

whole momentum range of 2-100 GeV, we would not be sensitive to the proton mass, making it harder to distinguish the protons. The kaon momentum region was selected to be 9-12 GeV, based off of Figure 5, which is about half of that of the protons, this is because kaons are about half as massive as protons.

### Protons with Changed masses and Proton mass, Momentum 18-24GeV

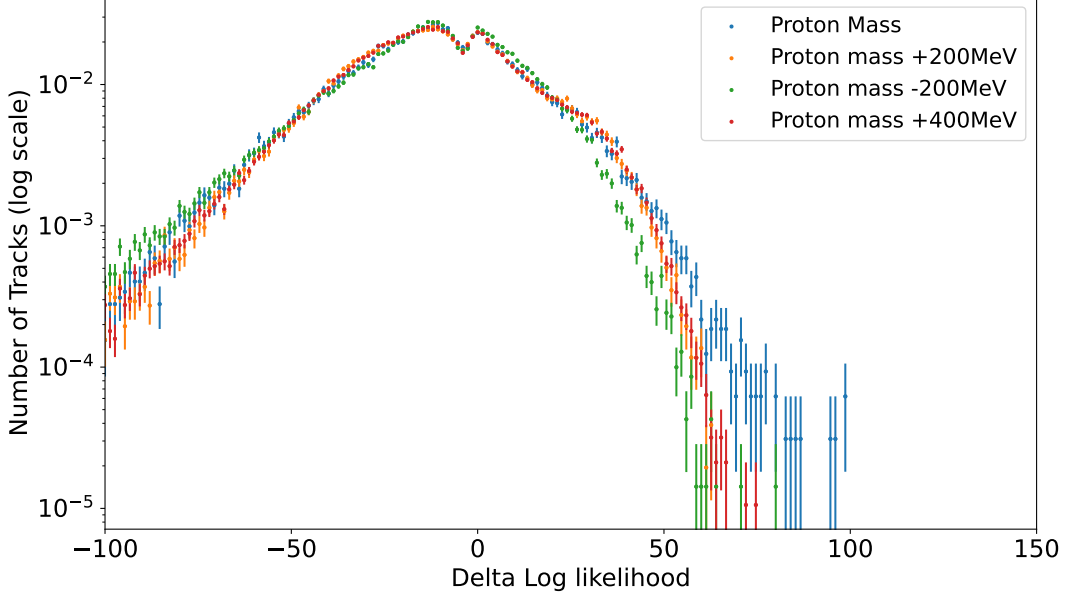


Figure 8: The number of tracks/frequency on a log scale versus the  $\Delta LL$  for protons at the proton mass and at the changed masses in the momentum region of 12-24 GeV. The plot has been normalised so that the area under graph is 1. Main peak centered around zero corresponds to pions, positive  $\Delta LL$  region shows peak for the protons at the expected proton mass in blue.

We can see that in Figure 8, there is an visible difference at the expected proton mass (blue curve) compared to the changed masses. This suggests that we are indeed likely detecting protons at the proton mass. The error bars were calculated based on Poisson statistics, so the uncertainty is taken to be the square root of the entries over the number of entries. Thus, they are larger where there are less entries, as can be seen in the positive  $\Delta LL$  region for the protons in Figure 8. The error bars suggest that our results are statistically significant as there is a visible difference with the unchanged proton mass to the changed masses considering the size of the error bars. We also have to remember that it is plotted on a log scale, so the difference that appears to be obvious with the proton mass is smaller than it actually appears in Figure 8.

As only a fraction of the 2018 data was used in these plots, if the rest of the data is used we expect that the error bars would be reduced in that region where we see the difference with the proton mass to the changed masses, more data would also make the overall difference that is present more distinct.

The changed mass of 200 MeV below the proton mass (green curve) appears to undershoot compared to the masses of 200 MeV and 400 MeV above the proton mass. This is likely because it is closer to the kaon mass which is roughly 490 MeV, while it is not at the actual kaon mass, it is likely that the kaons may still be having an effect, causing the results to be askew. This is because we are looking at probabilities, so it could be that kaon hypothesis becomes more probable. To resolve this, additional masses below the proton mass could be analysed and plotted for the  $\Delta LL$  for the protons to see in grater detail what is happening as the mass is lowered below the proton mass. We may also consider when applying the method to deuterons, to choose masses only above the deuteron mass.

The plot for the  $\Delta LL$  for kaons at the expected proton mass and at the changed masses in Figure

## Kaons with Changed masses and Proton mass, Momentum 9-12GeV

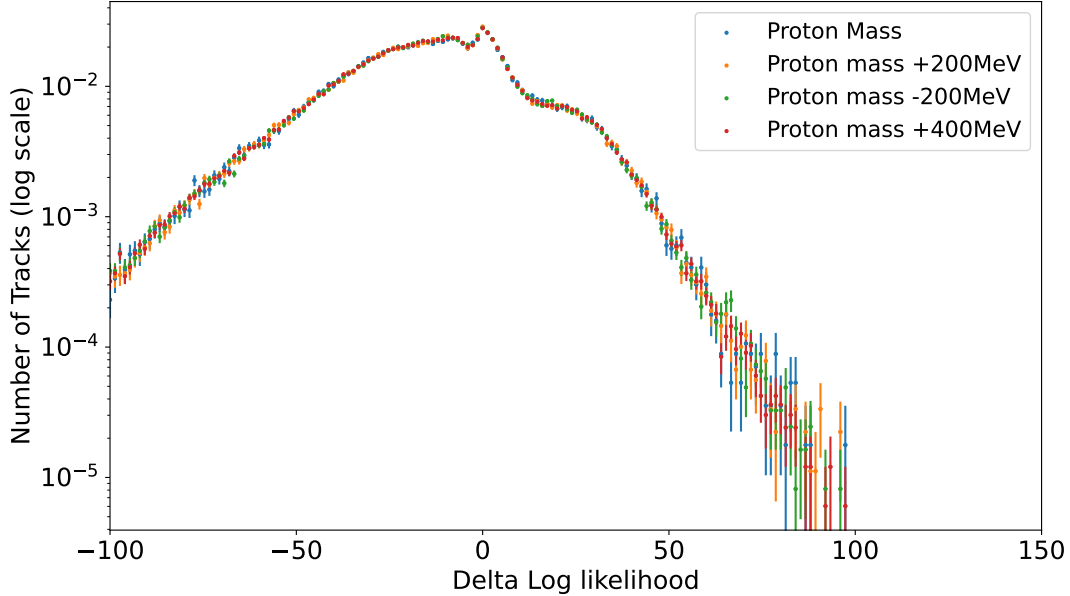


Figure 9: The number of tracks/frequency on a log scale versus the  $\Delta LL$  for kaons at the proton mass and at the changed masses in the momentum region of 9-12 GeV. The plot has been normalised so that the area under graph is 1. Main peak centered around zero corresponds to pions, positive  $\Delta LL$  region no peak at the proton mass nor changed masses.

9, appears to be unchanged compared to Figure 8. The expected proton mass (blue curve) does not seem to have that same obvious peak as we saw for the protons in Figure 8, nor does the mass of 200 MeV below the proton mass seem to undershoot.

The error bars included in Figure 9 were calculated also using Poisson statistics, like Figure 8, the error bars appear to be a lot larger in the higher  $\Delta LL$  region. This will also reduce in size with more data analysed. The lack of an obvious peak at the proton mass for the  $\Delta LL$  for kaons, further suggests that we are likely actually detecting protons in Figure 8 and not other random events or background.

Thus the method appears to be valid, as we can see an obvious peak corresponding to the protons, we may then be able to apply the same method to deuterons. We would do this by using the  $\Delta LL$  for deuterons at the expected deuteron mass and at other changed masses to see if we can get a similar peak at the deuteron mass compared to the changed masses as we saw for the protons. We expect that this peak would be a lot smaller as deuterons are about 1000 times rarer than protons, though we hope with more data that we may be able to detect a difference using the background.

## 5 Conclusion

This project developed a method for measuring protons detected at the LHCb detector by looking at the background near the proton mass. Deuterons cannot be measured directly on a case-by-case basis, nor could they be measured collectively with a Statistical approach. This motivated the idea of looking at the background, using the proton mass to first validate the method. The determination of the background at the masses of 200 MeV above and below the proton mass and 400 MeV above the proton mass showed the peak from the protons to be more visible, showing this method is valid. However, masses below the proton mass should be further looked into, given that the 200 MeV below the proton mass did not match the other changed masses, most likely due to it being closer to the Kaon mass. The fact that the protons could be distinguished from the background gives some confidence that the same method may be applied to the rarer deuterons using the same data set with a larger

quantity. It will be expected that the peak for the deuterons will be a lot smaller than the proton peak, thus a larger data set will also hopefully make the deuterons more distinguishable from the background.

## 6 Future Work

A larger fraction, or ideally all of the 2018 data should be further analysed to get a more noticeable difference between the changed proton mass and unchanged proton mass. This will then tell us with more confidence that protons are being detected, by further reducing the size of the error bars.

Once more data has been analysed, the hope is to then apply the same method to the deuterons, using hypothetical mass hypotheses above and below the deuteron mass, to see if we can get a similar peak as was seen for the protons using the same data set. These results could be improved even further with more data, such as from the expected 2022-2023 data taking run from the LHCb detector or any other future data. An even larger data set will hopefully greatly increase the visibility of the potential deuteron peak to the background. Giving more certainty that deuterons are being detected.

There is also hope in the future to calculate the number of protons being detected, and eventually the number of deuterons, as this will tell us how many anti-deuterons we need to look for in cosmic radiation, to try and indirectly detect dark matter.

## References

- [1] S. K. Baker, *Measurement of Deuterons at LHCb*, PhD thesis, Department of Physics, Imperial College London, 2019.
- [2] E. Walton, *Searching for (Anti-)Deuterons using the LHCb Detector*, Honours thesis, Department of Physics, Monash University, 2021.
- [3] M. Thomson, *Modern Particle Physics*, Cambridge University Press, 2013.
- [4] M. Schumann, *Direct Detection of WIMP Dark Matter: Concepts and Status*, J. Phys. G46 (2019) no.10, 103003, [arXiv:1903.06477](#).
- [5] R. Massey, T. Kitching, J. Richard, *The dark matter of gravitational lensing*, Rep. Prog. Phys. 73 (2010) 086901, [arXiv:1001.1739](#).
- [6] P. Salati, *Dark Matter Annihilation in the Universe*, World Scientific Pub Co Pte Lt 30 (2014) 1460256, [arXiv:1403.4495](#).
- [7] C. Arina, J. Hajer, and P. Klose, *Portal Effective Theories: A Framework for the Model Independent Description of Light Hidden Sector Interactions*, [arXiv:2105.06477](#).
- [8] CMS, A. M. Sirunyan *et al.*, *Search for invisible decays of a Higgs boson produced through vector boson fusion in proton-proton collisions at  $\sqrt{s} = 13$  TeV*, Phys. Lett. B 793 (2019) 520, [arXiv:1809.05937](#).
- [9] S. Giagu, *WIMP dark matter searches with the ATLAS detector at the LHC*, Frontiers in Physics 7 (2019) 75.
- [10] I. Sepp, *Using Rare Decays to Probe the Standard Model at LHCb*, PhD thesis, Blackett Laboratory, Imperial College London, 2014.
- [11] J. Tjemsland, *Formation of light (anti)nuclei*, PoS TOOLS2020 (2021) 006, [arXiv:2012.12252](#).
- [12] L. A. Dal and A. R. Raklev, *Alternative formation model for antideuterons from dark matter*, Phys. Rev. D 91 (2015) 123536, [arXiv:1504.07242](#), [Erratum: Phys.Rev.D 92, 069903 (2015), Erratum: Phys.Rev.D 92, 089901 (2015)].
- [13] F. Barile, *(Anti-)deuteron production at the LHC with the ALICE-HMPID detector*, 38 (2015) 64, [ncc10949](#)
- [14] ALICE Collaboration, S. Acharya *et al.*, *(Anti-)deuteron production in pp collisions at  $\sqrt{s} = 13$  TeV*, Eur. Phys. J. C 80 (2020) 889, [arXiv:2003.03184](#).
- [15] ALICE Detector, CERN, <https://home.cern/science/experiments/alice>, Accessed: 2/11/2022.
- [16] LHCb Collaboration, J. A. A. A Ives *et al.*, *The LHCb detector at the LHC*, Journal of Instrumentation 3 (2008) S08005.
- [17] J. D. Jackson, *Classical Electrodynamics, Third Edition*, John Wiley & Sons, Inc., 1999.
- [18] H. Alaeian, An Introduction to Cherenkov Radiation, <http://large.stanford.edu/courses/2014/ph241/alaecian2/>.
- [19] Particle Data Group, M. Tanabashi *et al.*, *Review of Particle Physics*, Phys. Rev. D 98 (2018) 030001.